Separation Science and Technology
Publication details, including instructions for authors and subscription information:
http://www.informaworld.com/smpp/title~content=t713708471

Kinetics of Mn(II) Transport from Aqueous Sulfate Solution through a Supported Liquid Membrane Containing Di(2-ethylhexyl) Phosphoric Acid in Kerosene

R. Mohapatra[a]; S. B. Kanungo[a]
[a] REGIONAL RESEARCH LABORATORY, BHUBANESWAR, ORISSA, INDIA

To cite this Article Mohapatra, R. and Kanungo, S. B.(1992) 'Kinetics of Mn(II) Transport from Aqueous Sulfate Solution through a Supported Liquid Membrane Containing Di(2-ethylhexyl) Phosphoric Acid in Kerosene', Separation Science and Technology, 27: 13, 1759 — 1773
To link to this Article: DOI: 10.1080/01496399208019445
URL: http://dx.doi.org/10.1080/01496399208019445

SEPARATION SCIENCE AND TECHNOLOGY, 27(13), pp. 1759–1773, 1992

Kinetics of Mn(II) Transport from Aqueous Sulfate Solution through a Supported Liquid Membrane Containing Di(2-ethylhexyl) Phosphoric Acid in Kerosene

R. MOHAPATRA and S. B. KANUNGO*
REGIONAL RESEARCH LABORATORY
BHUBANESWAR-751013, ORISSA, INDIA

Abstract

The permeation rate of Mn(II) from its aqueous sulfate solution through a solid supported liquid membrane containing di(2-ethylhexyl) phosphoric acid (D2EHPA) in kerosene as the mobile carrier has been studied as a function of hydrodynamic conditions, concentrations of Mn^{2+} (0.91–16.38 mol/m^3) and H^+ (pH 2.0–5.0) in the feed solution, carrier concentration (10–800 mol/m^3) in the membrane, and temperature. It is observed that as the Mn(II) flux approaches a plateau region, the rate of permeation is predominantly controlled by diffusion through the membrane. On the other hand, at low Mn(II) and high H^+ ion concentrations, the high diffusivity of the Mn-D2EHPA complex causes the overall permeation rate to be controlled by the interfacial reaction. It is also observed that the rate of Mn(II) permeation is first order with respect to dimer concentration up to 40 mol/m^3 and half order above this concentration. Kinetic equations derived on the basis of the proposed mechanism are found to fit the experimental data satisfactorily.

INTRODUCTION

In a previous communication (*1*) it was shown that the rate of permeation of Co(II) through a supported liquid membrane (SLM) containing di(2-ethylhexyl) phosphoric acid (D2EHPA) in kerosene is primarily controlled by diffusion through the aqueous boundary layer at a lower metal ion concentration and pH. However, the interfacial chemical reaction becomes rate controlling at high pH and D2EHPA concentration. Although D2EHPA has been used in the solvent extraction and separation of Mn(II) by a few investigators (*2–6*), no work has been reported on its use as a

*To whom correspondence should be addressed.

carrier in a liquid membrane for the transport of Mn(II). This aspect assumes particular importance because of the problem of separation of Mn(II) from other valuable metal ions such as Co(II), Ni(II), and Cu(II) that are present in the acidic leach liquor of manganese nodules. The object of the present work is to investigate the kinetics and mechanism of the transport of Mn(II) through a liquid membrane containing D2EHPA in a kerosene medium.

THEORETICAL CONSIDERATIONS

Our experimental results (as shown in later sections) reveal that Mn(II) flux across a D2EHPA–kerosene liquid membrane is first order with respect to low Mn concentrations in the feed solution. It is also observed that Mn(II) flux is first and half order with respect to D2EHPA at lower (<150 mol/m^3) and higher (>150 mol/m^3) concentrations, respectively. Further, the very high diffusion of Mn(II) through the membrane suggests that the diffusing species is of low molecular weight, and this accounts for the high flux rate of Mn(II) compared to Co(II). Therefore, the following mechanism is proposed for Mn(II) transport through a D2EHPA–kerosene membrane.

Step I. The combined effects of the following three fast interfacial reactions generate negatively charged ligand species at the aqueous–organic interface.

$$(a)\ \overline{(HL)_2} \xrightarrow{1/k_2} 2\overline{(HL)}$$

$$(b)\ \overline{(HL)} \xrightarrow{K_d} \overline{(HL)}$$

$$(c)\ (HL) \xrightarrow{K_a} H^+ + L^-$$

Step II. The reaction of Mn^{2+} at the interface with the ligand species depends upon the pH and concentration of the ligand.

$$Mn^{2+} + L^- \xrightarrow{K_{II}} MnL^+$$

Step III. The formation of neutral Mn(II) species at the aqueous feed side of the interface.

$$MnL^+ + \overline{(HL)} \xrightarrow{K_{III}} MnL_2 + H^+$$

Step IV. The dissolution of the neutral species in the organic phase, which is a fast process.

$$MnL_2 \xrightarrow{K_{IV}} \overline{(MnL_2)}$$

Obviously, either Step II or Step III is a slow process controlling the overall rate of mass flux across the membrane. It is proposed that at a lower concentration of D2EHPA and at a lower pH, the interface remains largely saturated with $(\overline{HL})$, and Step II is a slower process compared to Step III. Conversely, at a higher concentration of D2EHPA and at a higher pH, the interface tend to become saturated with L^- and therefore Step III tends to be a rate-controlling process.

Case I: If Step II is a slow process, we may formulate

$$\text{Rate of forward reaction } (R_f) \propto [Mn^{2+}]_i[L^-]$$
$$\text{Rate of backward reaction } (R_b) \propto [MnL^+]_i$$

Combining different reactions under Step I, we have

$$[L^-] = K'[(HL)_2]^{\frac{1}{2}}/[H^+]$$

where

$$K' = K_a/K_d(K_2)^{\frac{1}{2}}$$

Therefore, combining Steps I and II on one hand and Steps III and IV on the other, the resulting rate of reaction at the interface (R_0) may be written as

$$R_0 = R_f - R_b$$

$$R_0 = \frac{k_1[Mn^{2+}]_i\overline{[(HL)_2]}}{[H^+]} - k_{-1}[\overline{MnL_2}][H^+] \tag{1}$$

Case II: If Step III is a slow process, it can be similarly shown that

$$R_0' = \frac{k_1'[Mn^{2+}]_i\overline{[(HL)_2]}^{\frac{1}{2}}}{[H^+]} - k_{-1}'[\overline{MnL_2}][H^+] \tag{2}$$

As in the case of any liquid membrane process, we have for diffusion through an aqueous film

$$J_w = \frac{1}{\Delta_a}\{[Mn^{2+}]_b - [Mn^{2+}]_i\} \tag{3}$$

and for mass transport (diffusional) through a membrane

$$J_m = \frac{1}{\Delta_0}[\overline{MnL_2}] \tag{4}$$

where Δ_a and Δ_0 are the coefficients of mass transfer through an aqueous film and a membrane, respectively.

Since at steady state $R_0 = J_w - J_m = J$, by combining Eqs. (1), (3), and (4) on one hand and Eqs. (2), (3), and (4) on the other, we may split the overall flux (J) equation into the three following rate-limiting cases on the basis of relative resistance ($1/J$) of each process (*7*, *8*).

(i) Aqueous film diffusion:

$$J = [Mn^{2+}]/\Delta_a \tag{5}$$

(ii) Membrane diffusion:

$$J = \frac{K_{ex}[Mn^{2+}][\overline{(HL)_2}]}{\Delta_0[H^+]^2} \tag{6}$$

$$J' = \frac{K_{ex}[Mn^{2+}][\overline{(HL)_2}]^{\frac{1}{2}}}{\Delta_0[H^+]^2} \tag{7}$$

where K_{ex} is the equilibrium constant (k_1/k_{-1}) to be determined by the solvent extraction method.

(iii) Interfacial chemical reaction:

$$J = \frac{k_1[Mn^{2+}][\overline{(HL)_2}]}{[H^+]} \tag{8}$$

$$J' = \frac{k_1'[Mn^{2+}][\overline{(HL)_2}]^{\frac{1}{2}}}{[H^+]} \tag{9}$$

Since the concentration of monomer is negligibly small in kerosene, the total analytical concentration of D2EHPA within the membrane may be given by

$$C_t = 2[\overline{(HL)_2}] + 2[\overline{MnL_2}]$$

The above flux equations for different rate-controlling processes may now be written in terms of C_t. Thus, Eqs. (6) and (7) are transformed into Eqs. (10) and (11), respectively:

$$J = \frac{1}{\Delta_0} \frac{C_t\alpha}{2(\alpha + 1)} \tag{10}$$

$$J' = \frac{\alpha}{2\Delta_0}\{(\alpha^2 + 2C_t)^{\frac{1}{2}} - \alpha\} \tag{11}$$

where

$$\alpha = \frac{K_{cx}^m[Mn^{2+}]}{[H^+]^2}$$

and K_{cx}^m is the equilibrium constant within the membrane phase and is obtained by dividing K_{cx} by the porosity of the membrane. Similarly, Eqs. (8) and (9) are transformed into Eqs. (12) and (13), respectively:

$$J = \frac{C_t}{2(\Delta_0\beta + 1)} \tag{12}$$

$$= \frac{\beta}{2}[(\Delta_0\beta)^2 + 2C_t)^{\frac{1}{2}} - \Delta_0\beta] \tag{13}$$

where $\beta = k_1[Mn^{2+}]/[H^+]$.

EXPERIMENTAL

Materials

All reagents such as $MnSO_4 \cdot H_2O$, anhydrous Na_2SO_4, CH_3COONa, CH_3COOH, etc. used in the present work were of analytical grade. D2EHPA, of 99% purity (K and K, USA), was used without any further purification. Distilled kerosene (bp 170–220°C) was used as a diluent.

Membrane

Microporous polypropylene membrane Celgard 2500 was used as a solid support. The characteristics of the membrane were mentioned in our earlier communication (*1*).

Method

The details of the diffusion cell system and the experimental procedure were described in our previous communication (*1*). The aqueous feed solution consists of a Mn^{2+} concentration ranging from 0.910 to 18.5 mol/m^3; 9 mol/m^3 Na_2SO_4, and 5 mL acetate buffer per 100 mL. The pH of the feed solution varied from 2.0 to 4.5. The stripping solution consists of 900 mol/m^3 H_2SO_4.

Solvent Extraction

To determine the equilibrium constant of extraction, equal volumes of known concentrations of manganese solution in water and D2EHPA in kerosene were taken in a separating funnel and thoroughly shaken for 20 min at 303 K. After equilibration, the Mn(II) was estimated in the aqueous phase and its equilibrium pH was noted.

RESULTS AND DISCUSSION

Mn(II) flux across the membrane was calculated from the slope of the initial (up to 5 h) linear plot of Mn(II) concentration in the stripping compartment against time according to the following relationship:

$$J = \frac{V}{A}\frac{d[\mathrm{Mn(II)}]}{dt} \ \mathrm{mol \cdot m^{-2} \cdot s^{-1}}$$

where V = volume of solution in each side of the membrane (m^3)
A = effective membrane area (m^2)

The following parameters were studied in order to elucidate the kinetics and mechanism of Mn(II) permeation across the D2EHPA–kerosene membrane.

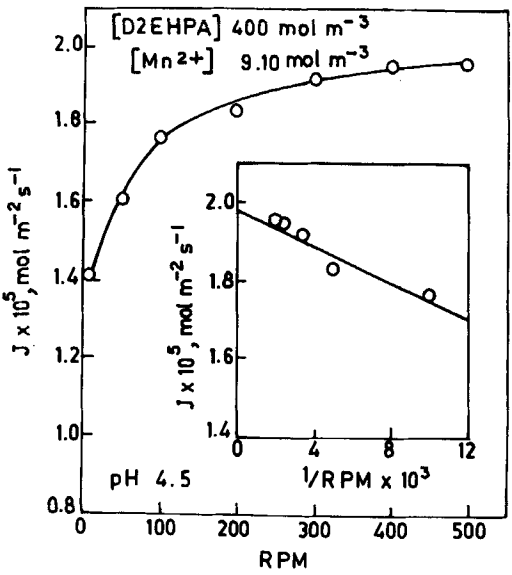

FIG. 1. Variation of J with an increase in the stirring rate of the solution. The inset shows J versus the reciprocal of rpm.

Effect of Stirring Rate

The effect of stirring rate on Mn(II) flux is illustrated in Fig. 1 which shows that the typical plateau region is reached at a stirring rate above 400 rpm where the diffusional resistance due to the stagnant aqueous boundary layer is minimum. The inset figure shows that at infinitely high agitation the maximum flux is 1.985×10^{-5} mol·m^{-2}·s^{-1}, which is close to the 1.95×10^{-5} mol·m^{-2}·s^{-1} found at 400–500 rpm. Consequently, all subsequent experiments were carried out at a stirring rate of 450 rpm.

However, the limiting value of J in the plateau region depends upon the concentration of metal ions in the feed solution. A simple plot of J against the concentration of Mn(II) shows a direct linear relationship up to 3.0 mol/m^3 (figure not shown). The slopes of the straight lines give an average value of 0.215×10^6 s/m as the aqueous film mass transfer coefficient (Δ_a).

Effect of H^+ Ion Concentration

The effect of H^+ ion concentration on Mn(II) flux at two different concentrations of Mn(II) is illustrated in Fig. 2 in the form of a log-log plot. The low flux rate at high $[H^+]$ is due to low acid dissociation of monomer at the aqueous feed–organic interface. Under this condition the rate of permeation is controlled by the interfacial chemical reaction. As

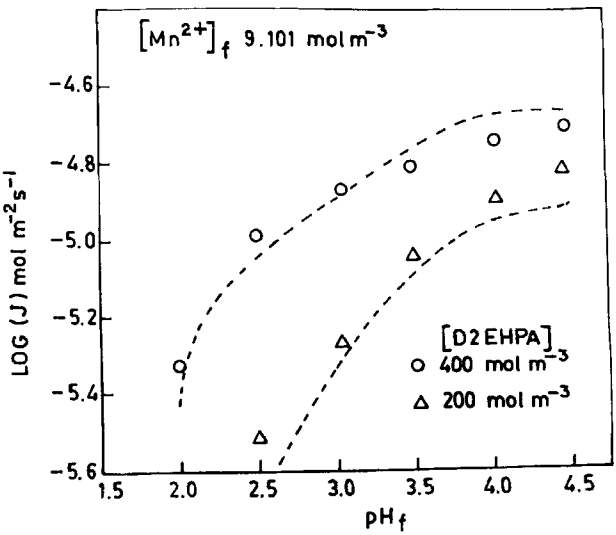

FIG. 2. Change in J with an increase in the pH of the feed solution. The broken lines show the change in flux values calculated from Eq. (13). For low concentrations of Mn^{2+} (<2.0 mol/m^3), a combination of Eqs. (5) and (13) was used.

$[H^+]$ decreases, the rate of interfacial chemical reaction increases, and therefore either diffusion through the aqueous boundary layer or through the membrane or both tend to become rate controlling. The plateau region attained at higher pH is due to gradual saturation of the organic phase with the Mn-D2EHPA complex. Under the circumstances, membrane diffusion is unlikely to be the rate-controlling step, and the interfacial chemical reaction becomes rate controlling.

Combining Eqs. (5) and (9) and transposing, we have

$$\frac{[Mn^{2+}]}{J} = \Delta_a + \frac{[H^+]}{k_1[(\overline{HL})_2]^{\frac{1}{2}}} \tag{14}$$

Figure 3 is a plot of $[Mn^{2+}]/J$ vs $[H^+]$ for two different dimer concentrations. The figure demonstrates that a better linear relationship is observed for 100 mol/m^3 of $[(\overline{HL})_2]$ than for 200 mol/m^3, suggesting that the interfacial chemical reaction becomes rate controlling when the organic phase tends to become saturated with the Mn(II)-D2EHPA complex. However, from the slopes of the two different straight lines, two different k_1 and k_{-1}

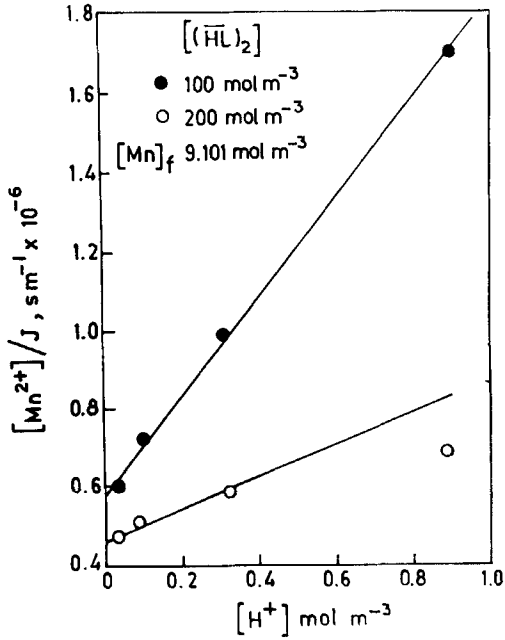

FIG. 3. Plot of $[Mn^{2+}]/J$ versus $[H^+]$ according to Eq. (14) using the data from Fig. 2.

values were obtained. By using these values of k_1 and their corresponding dimer concentrations, J values were calculated from Eq. (13).

The calculated values of J are lower than those found experimentally, but when the mass transfer coefficients due to aqueous film diffusion as obtained from the intercepts of Fig. 3 are taken into account, the calculated values of J fit satisfactorily with those found from experiments. The broken lines in Fig. 2 show the calculated values of flux as a function of pH.

Effect of Mn(II) Concentration

Figure 4 depicts the effect of Mn(II) concentration in the feed solution at pH 4.45 on metal ion flux across a membrane containing three different concentrations of D2EHPA in kerosene. It can be seen from the figure that at a low concentration of Mn(II) (up to 2.73 mol/m^3) the flux is first order with respect to Mn(II) concentration. As the Mn(II) concentration increases, the interfacial reaction rate becomes faster and the membrane phase tends to become saturated with the metal complex. Further, the concentration gradient between the bulk and the aqueous boundary layer sharply diminishes. All these factors lead to a limiting plateau region of metal ion flux across the membrane.

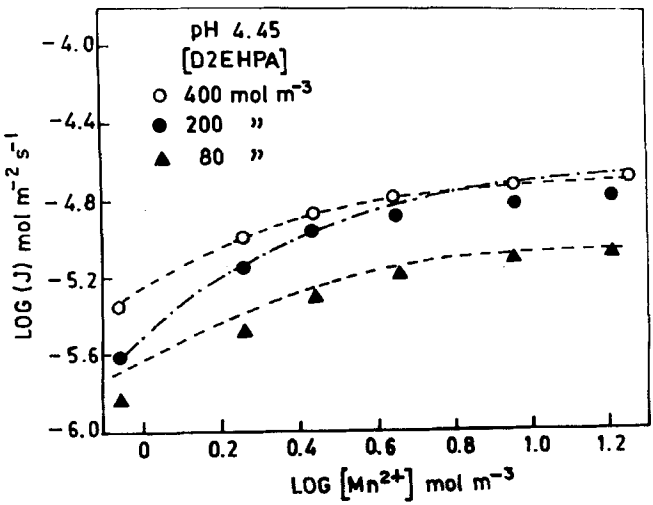

FIG. 4. Log-log plot of J versus [Mn^{2+}] in the feed solution. The broken lines represent the J values calculated from a combination of Eqs. (5) and (11) up to [Mn^{2+}] of 4.0 mol/m^3 and Eq. (11) alone above that concentration. For [D2EHPA] of 80 mol/m^3, a combination of Eqs. (11) and (13) shows a better fit.

Under such limiting conditions, diffusion through the membrane becomes rate controlling and Eq. (7) becomes

$$J'_{\text{lim}} = \frac{1}{\Delta_0} \frac{[\overline{(MnL_2)}]}{[\overline{(HL)_2}]^{\frac{1}{2}}} \tag{15}$$

since in the kerosene solution the concentration of monomer is negligibly small (*1*). We have

$$C_t = 2[\overline{(HL)_2}] + 2[\overline{MnL_2}] \tag{16}$$

or

$$[\overline{(HL)_2}]^{\frac{1}{2}} = \sqrt{\frac{C_t}{2}} \left(1 - \frac{2\overline{(MnL_2)}}{C_t}\right)^{\frac{1}{2}} \tag{17}$$

Using binomial expansion and neglecting terms higher than square,

$$[\overline{(HL)_2}]^{\frac{1}{2}} = \sqrt{\frac{C_t}{2}} \left\{1 - \frac{1}{2}\left(\frac{2[\overline{MnL_2}]}{C_t}\right) - \frac{1}{8}\left(\frac{2[\overline{MnL_2}]}{C_t}\right)^2\right\}$$

Since at the limiting state $C_t = 2[\overline{MnL_2}]$,

$$[\overline{(HL)_2}]^{\frac{1}{2}} = \frac{3}{8}\sqrt{\frac{C_t}{2}} \tag{18}$$

and therefore Eq. (15) becomes

$$J'_{\text{lim}} = \frac{1}{\Delta_0} \frac{\sqrt{C_t}}{0.53} \tag{19}$$

Figure 5 shows the plot of log J'_{lim} values obtained from Figs. 1, 2, 4, and 6 against log C_t. The slope of the resultant straight line is 0.5, which agrees with Eq. (19). From the intercept, Δ_0 is found to be 0.188×10^7 s/m.

In order to confirm the diffusion-controlled mechanism for the variation of Mn(II) concentration, we calculated flux values for different concentrations of Mn(II) using both Eqs. (10) and (11). While Eq. (10) is found to be valid only for very low concentrations (<2.0 mol/m^3), Eq. (11) exhibits a better fit for the entire range of concentrations using Δ_0 values

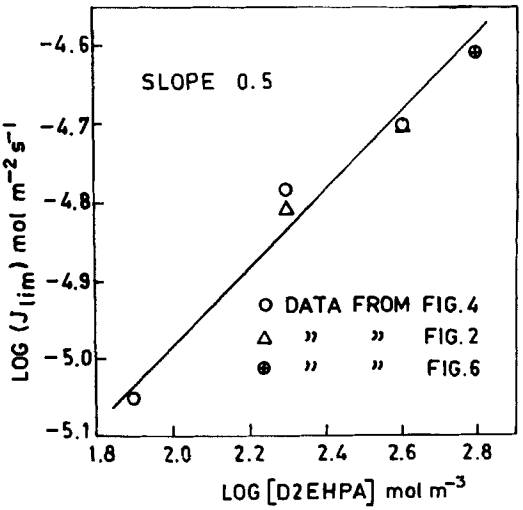

FIG. 5. Relationship between limiting values of J and total [D2EHPA] concentration.

of 0.55×10^7 s/m instead of 0.188×10^7 s/m as obtained from Eq. (19). The former value was obtained from Fig. 7 for the variation of D2EHPA concentration as discussed in the following section. However, a closely similar value of Δ_0 can be obtained if 1.53 is used as the number in the denominator of Eq. (19), suggesting that this number represents the sum of stoichiometric coefficients of the reactions of D2EHPA with Mn(II).

The mechanism, however, changes as the concentration of D2EHPA is decreased to 80 mol/m^3. As the concentration of manganese is increased, a combination of Eqs. (11) and (13) satisfactorily follows the observed flux values, as shown in Fig. 4. Indeed, at a 200 mol/m^3 D2EHPA concentration the combination of the above two equations fits better than does Eq. (11) alone at Mn^{2+} concentrations higher than 10 mol/m^3.

Effect of D2EHPA Concentration

Figure 6 illustrates the log-log relationship between the concentration of dimer $[\overline{(HL)_2}]$ and Mn(II) flux across the membrane at two different Mn(II) and hydrogen ion concentrations. The figure shows that at dimer concentrations below 30 mol/m^3 the linear relationship gives a slope of 1.0 while above this concentration the slope value is about 0.50. This further supports the mechanism of Mn(II) transport across the D2EHPA–kerosene membrane as proposed in earlier sections.

It now appears that both the mass transfer and the interfacial chemical reaction control the rate of Mn(II) transport. First, consider diffusional

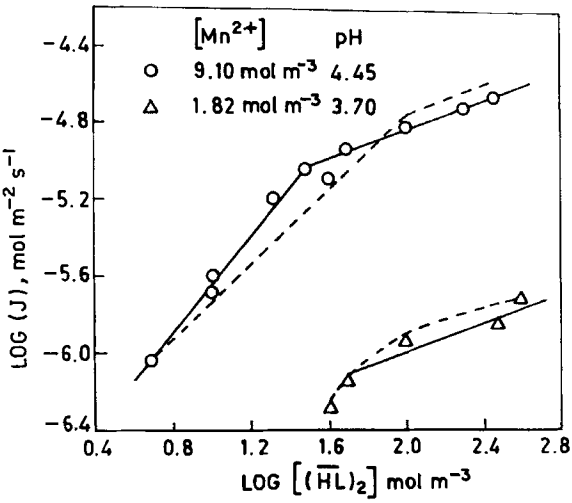

FIG. 6. Log-log relationship between J and the concentration of the dimer. Broken lines represent J values calculated from Eq. (13).

mass transfer as a function of dimer concentration. Combining both aqueous film and membrane diffusion phenomena as envisaged in Eqs. (5)–(7) and rearranging, we have

$$\frac{[Mn^{2+}]}{[H^+]J} = \frac{\Delta_a}{[H^+]} + \frac{[H^+]\Delta_0}{K_{ex}^m[(\overline{HL})_2]^n} \tag{20}$$

where n is the stoichiometric coefficient which is assumed to be 2, 1, or $\frac{1}{2}$. Figure 7 plots the left-hand side of Eq. (20) against $1/[(\overline{HL})_2]^n$. It can be seen from the figure that for $n = 2$, no linear relationship is obtained and therefore this value can be rejected. For $n = 1$, a good linear relationship is obtained from high to low concentrations of dimer, whereas for $n = \frac{1}{2}$ the linear relationship is followed from 300 to 50 mol/m^3 of $[(\overline{HL})_2]$. The two linear relationships yield two different values of Δ_0 and Δ_a. Since at higher dimer concentrations an order of $\frac{1}{2}$ has already been established, we have taken the value of Δ_0 obtained from the slopes of the linear portion of the plot for $n = \frac{1}{2}$. It can be seen from Table 1 that the value of 0.55×10^7 s/m is higher than that obtained from Fig. 5.

At both low Mn(II) concentrations and pH values of the aqueous feed solution, a linear relationship is followed only for $n = \frac{1}{2}$, as illustrated in Fig. 8. The Δ_0 value obtained under these conditions in 0.0913×10^7 s/m, indicating a very high rate of diffusion through the membrane. Consequently, the interfacial chemical reaction rate controls Mn(II) flux across the membrane.

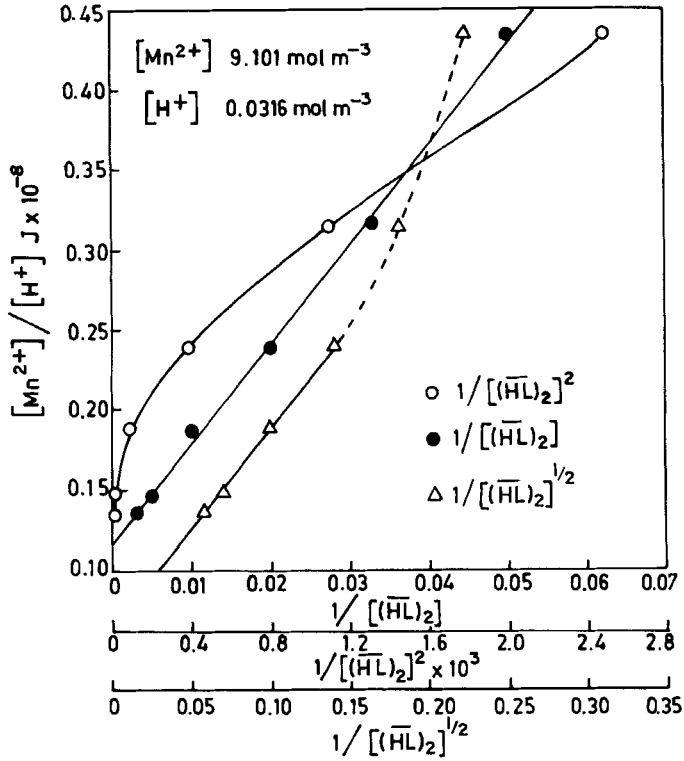

FIG. 7. Plot of $[Mn^{2+}]/J[H^+]$ versus $1/[\overline{(HL)_2}]^n$ for $n = 2$, 1, and $\frac{1}{2}$.

TABLE 1
Kinetic Parameters for the Permeation of Mn(II) through Solid Supported D2EHPA–Kerosene Liquid Membrane

Model equations	Δ_a (s/m)	Δ_0 (s/m)	k_1 ($m^4 \cdot mol^{-1} \cdot s^{-1}$)	k_1 ($m^4 \cdot mol^{-1} \cdot s^{-1}$)[a]	K_{ex}^m
Eq. 5	0.20×10^6				1.55×10^{-3}
	0.235×10^6				
Eq. (20) for $n = \frac{1}{2}$	0.187×10^6	0.55×10^7			
Eq. (20) for $n = 1$	0.414×10^6				
From limiting values, $\log C_t \rightarrow \alpha$ and $\log H^+ \rightarrow -\alpha$	0.414×10^6	0.187×10^7			
Eq. (14)			16.64×10^{-8}	1.073×10^{-4}	
			7.81×10^{-8}	0.538×10^{-4}	

[a] $k_{-1} = k_1/K_{ex}^m$.

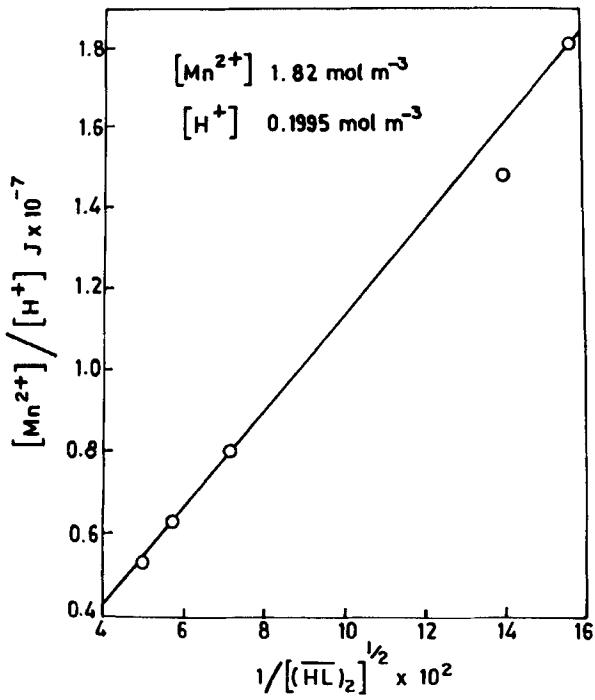

FIG. 8. Plot of $[Mn^{2+}]/J[H^+]$ versus $1/[\overline{(HL)_2}]^{\frac{1}{2}}$ using the data of Fig. 6 for low $[Mn^{2+}]$ concentration.

In order to confirm the above conclusion, flux values were calculated to test whether the experimental data in Fig. 6 fit either the diffusion or chemical reaction controlled model. It has been observed that at high concentrations of Mn(II) and higher pH values, both Eqs. (12) and (13) yielded similar calculated values of J. At both low Mn(II) concentrations and pH values, however, only Eq. (13) fits the experimental data well. The values of J calculated from these equations are shown in Fig. 6 as broken lines which clearly demonstrate that the interfacial chemical reaction is rate controlling either at high Mn^{2+} or high D2EHPA concentrations.

Effect of Temperature

Mn(II) flux across a supported liquid membrane containing 400 mol/m^3 of D2EHPA in kerosene has been determined at four different temperatures: 303, 313, 323, and 333 K. The initial concentration of Mn^{2+} and the pH value in the feed solutions were 9.10 mol/m^3 and 4.5, respectively. An Arrhenius-type plot (figure not shown) is followed perfectly only in the 303–323 K temperature range. The apparent activation energy is found to

be 12.1 kJ/mol, which shows that under the above experimental conditions the rate of transport is predominantly controlled by a mass-transfer (diffusion) mechanism.

NOMENCLATURE

J	Mn(II) flux ($mol \cdot m^{-2} \cdot s^{-1}$)
J_{lim}	Mn(II) flux at limit $\log C_t \rightarrow \alpha$ and $\log H^+ \rightarrow -\alpha$
k_1	forward reaction rate ($m^4 \cdot mol^{-1} \cdot s^{-1}$)
k_{-1}	backward reaction rate ($m^4 \cdot mol^{-1} \cdot s^{-1}$)
K_{ex}	equilibrium constant
K_{ex}^m	equilibrium constant in membrane
ϵ	porosity of the membrane
t	time (s)
Δ_a	mass transfer coefficient in aqueous film diffusion (s/m)
Δ_0	mass transfer coefficient in membrane diffusion (s/m)
$\overline{(HL)_2}$	dimerized D2EHPA

Subscripts

b	bulk concentration
i	feed aqueous solution or the species adjacent to the interface between the feed solution and the membrane
—	species in organic medium

Acknowledgments

The authors wish to thank Dr. R. P. Das, Head of the Hydrometallurgy Division, for his keen interest and support. Thanks are also due to the director, R. R. L. Bhubaneswar, for his kind permission to publish this work. One of the authors (R.M.) is grateful to the Department of Ocean Development, Government of India, for the award of a fellowship.

REFERENCES

1. R. Mohapatra, S. B. Kanungo, and P. V. R. B. Sarma, *Sep. Sci. Technol., 27,* 765 (1992).
2. S. Jinglan, J. Dehua, and S. Sixiu, *Gaodeng Xuexiao Husaxue Xuebao, 5,* 7 (1984); *Chem. Abstr., 100,* 127567d (1984).
3. S. Sixiu, G. Zili, J. Dehua, and S. Jinglan, *Shandong Daxue Xuebao Ziran Kexueban, 1,* 75 (1985); *Chem. Abstr., 103,* 184629m (1985).
4. F. Islam and G. L. Deb, *J. Sci. Ind. Res. (Bangladesh), 9,* 85 (1974).
5. G. M. Ritcey and B. H. Lucas, *Can. Met. Q., 10,* 223 (1971).
6. G. M. Ritcey and A. W. Ashbrook, U.S. Patent 3,339,055 (August 1968).
7. P. R. Danesi, *Sep. Sci. Technol., 19,* 857 (1984).
8. I. Komasawa, T. Otake, and T. Yamashita, *Ind. Eng. Chem., Fundam., 22,* 127 (1983).

Received by editor September 5, 1991